Soft Matter

Growth of Form in Thin Elastic Structures

Journal:	*Soft Matter*
Manuscript ID	SM-ART-06-2018-001136.R2
Article Type:	Paper
Date Submitted by the Author:	17-Sep-2018
Complete List of Authors:	Al-Mosleh, Salem; University of Massachusetts Amherst, Physics Gopinathan, Ajay; University of California, Merced, School of Natural Sciences Santangelo, Christian; UMass Amherst, Physics

SCHOLARONE™
Manuscripts

Growth of Form in Thin Elastic Structures

Salem Al Mosleh[1], Ajay Gopinathan[2],* and Christian Santangelo[1†]
Department of Physics, University of Massachusetts Amherst, Amherst, MA 01003, USA[1] *and*
Department of Physics, University of California Merced, Merced, CA 95343, USA[2]

Heterogeneous growth plays an important role in the shape and pattern formation of thin elastic structures ranging from the petals of blooming lilies to the cell walls of growing bacteria. Here we address the stability and regulation of such growth, which we modeled as a quasi-static time evolution of a metric, with fast elastic relaxation of the shape. We consider regulation via coupling of the growth law, defined by the time derivative of the target metric, to purely local properties of the shape, such as the local curvature and stress. For cylindrical shells, motivated by rod-like E. *coli*, we show that coupling to curvature alone is generically linearly unstable to small wavelength fluctuations and that additionally coupling to stress can stabilize these modes. Interesting, within this framework, the longest wavelength fluctuations can only be stabilized with the mean curvature flow. Our approach can readily be extended to gain insights into the general classes of stable growth laws for different target geometries.

I. INTRODUCTION

How physical processes establish the growth and form of biological structures was considered by D'Arcy Thomson almost a century ago [1]. Since then, there has been much progress explaining the different growth driven morphologies that appear in the natural world. These include understanding that the rippled edges of leaves [2], the ruffled petals of blooming lilies and other flowers [3, 4], and even the convolutions of the brain cortex may be driven by differences in growth rate between spatially distinct regions [5]. It is well known that heterogeneous insertion and deletion of material can lead to geometric frustration and shape change in (synthetic) tissues [6–9]. Yet one hundred years after D'Arcy Thomson's seminal work, there are still challenges and open problems. One such challenge is that of determining the connection between the dynamical growth law —where a tissue chooses to grow —and both the shape and stability of those tissues.

This raises the question of how growth laws are regulated in nature to ensure stable growth. Feedback is a commonly used mechanism in biology for ensuring stability, but it is not clear to what or how the growth laws need to be coupled, to ensure the robust growth of a stable structure. A particular example of this issue is the question of shape regulation in rod-like *E. coli*, which is still an open problem [10, 11]. Though the components of the molecular machinery responsible for cell wall growth and regulation have been identified [12], precisely how the nm-scale components within this network interact to produce a robust shape at the μm-scale is not completely understood. Feedback between cell wall insertion rate and curvature, which was shown to be present in *E. coli* [13], can in principle lead to stable cylindrical shapes. However, as demonstrated in Refs. [14] and [15], stress also affects cell wall insertion rate and can lead to growth which is different from what would be expected from a purely geometric coupling.

Coupling growth to stress and geometry has been considered in other biological contexts as well. In the context of the fruit fly *Drosophila melanogaster*, Ref. [16] explored a mechanism for regulating growth through stress feedback. In plant growth, the Ricci flow [25] has in been studied in Ref. [17].

In this paper, we step back from the microscopic details of the growth process and consider a general framework for describing the growth of thin elastic structures that allows us to study stability. We assume that throughout the growth process, the material retains uniform thickness and Young's modulus. That is to say, it is still made of the same stuff, there is just more of it in some places and less in others. Mathematically, this growth process can be described as a change in the target metric of the shell or, alternatively, as the change in the local equilibrium lengths between points along the surface [7]. There are, of course, many ways that the target metric could change in time.

Here we consider regulating the growth by coupling the growth laws to purely local properties of the shape, such as the local curvature and stress. It is then possible to use considerations of symmetry and locality to make a curvature expansion and reduce the growth laws to only a few effective parameters. Our approach thus allows us to study the relationship between geometry and stress in determining the morphological stability of growing structures. Partially motivated by E. coli and partially for concreteness, we use our formalism to address the linear stability of elongating, cylindrical shapes as an example. Nevertheless, we develop principles that can be applied to morphology selection and stability in biological systems more generally.

This paper is organized as follows. In Sec. (II), we give a short overview of the required differential geometry. The purpose of this section is to give notation and definitions used in the other sections. In Sec. (III) we consider the energetics of thin elastic shells. In section

*e-mail: agopinathan@ucmerced.edu
†e-mail: csantang@physics.umass.edu

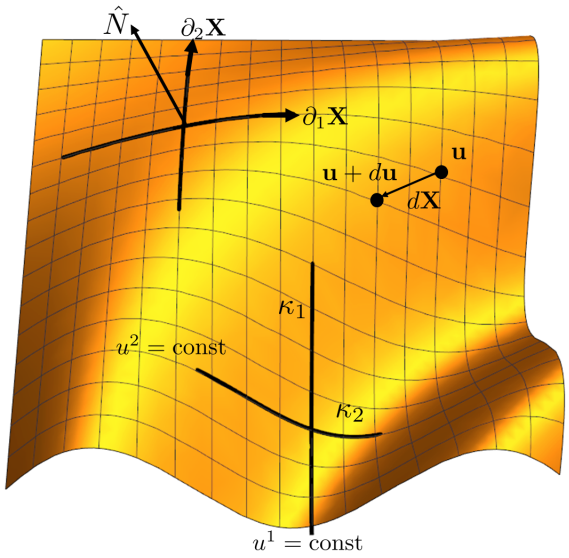

FIG. 1: (Color Online) u^1 and u^2 are the (arbitrary) coordinates chosen to parametrize the surface. Curves with constant coordinate values are shown. The vector $d\mathbf{X}$ is the displacement vector between the points parametrized by $\mathbf{u}$ and $\mathbf{u}+d\mathbf{u}$. The displacement vector satisfies $|d\mathbf{X}|^2 = d\ell^2$, which leads to the definition in Eq. (1). The unit vector $\hat{N}$ is normal to the surface at every point. We also show here the principal curvatures κ_1 and κ_2 defined roughly as the eigenvalues of the curvature tensor.

(IV) we describe the growth process, and show how symmetry can help us organize the different possible growth laws. This section provides the expression for the growth law, which is the first main contribution of this paper and will be used for the analysis of later sections.. Sec. (V) studies the stability of elongating cylindrical shapes. After showing that purely geometric coupling alone is generically linearly unstable to small wavelength fluctuations, we add the effect of coupling growth to stress and show that stability requires a combination of coupling to both curvature and stress. This represents the other main contribution of the paper. Finally, we conclude in Sec. (VI).

II. NOTATION AND DEFINITIONS

To establish notation and definitions, we give a brief overview of the differential geometry of surfaces in three dimensions. For a more detailed exposition, see [18, 19].

Throughout this paper we assume Einstein's summation convention, where repeated indices are summed unless otherwise stated. A surface embedded in 3D Euclidean space can be represented as a vector function of two variables, $\mathbf{X}(u^1, u^2) \equiv \mathbf{X}(\mathbf{u})$, as in Fig. (1). Information about the shape of the surface is encoded in the length and curvature of curves $\mathbf{u}(\ell)$ on the surface, parametrized by their arc length ℓ. The length of any curve can be determined from the metric tensor, g_{ij}, through the relation

$$d\ell^2 = (\partial_i\mathbf{X}\cdot\partial_j\mathbf{X})\, du^i du^j \equiv\ g_{ij}\, du^i du^j \tag{1}$$

where ∂_i is the partial derivative with respect to the coordinate u^i. Likewise the curvature tensor, b_{ij}, determines the curvature of curves in the direction normal to the surface through the relation (Fig. 1)

$$\kappa_N \equiv (\partial_i\partial_j\mathbf{X}\cdot\hat{N})\,\frac{du^i}{d\ell}\frac{du^j}{d\ell} \equiv b_{ij}\,\frac{du^i}{d\ell}\frac{du^j}{d\ell}. \tag{2}$$

The definition of the Gaussian, K, and mean, H, curvatures can be given by

$$2H \equiv g^{ij}\, b_{ij} \quad \text{and} \quad K \equiv \frac{\det(b_{ij})}{\det(g_{ij})}, \tag{3}$$

where g^{ij} is the matrix inverse of the metric g_{ij}, implying $g^{ij}g_{jk} = \delta^i{}_k$. Finally, note that by considering the matrix $b^i_j \equiv g^{ik}b_{kj}$, we can define two principle curvatures, κ_1 and κ_2, as the eigenvalues of b^i_j along with their associated principle directions. These principle curvatures represent maximal and minimal normal curvatures of curves passing through a point and, thus, they are coordinate invariants. They are related to the Gaussian and mean curvatures through the relations $K = \kappa_1\kappa_2$ and $2H = \kappa_1 + \kappa_2$.

It is well known that, if g_{ij} and b_{ij} satisfy compatibility conditions expressed through the Gauss-Codazzi-Mainardi equations, then they are sufficient to uniquely determine the surface up to rigid transformations. In that sense, we have a complete characterization of any surface in three dimensions from g_{ij} and b_{ij} alone.

Finally, we will give definitions of the metric and curvature strains which are relevant for elasticity. In addition to the metric we defined, which gives the actual lengths of curves on the surface, we can define what is called a target metric, $\bar{g}_{ij}$, which represents the "preferred" lengths of curves on a surface. In other words, when $g_{ij} = \bar{g}_{ij}$ all curves are unstretched. We can define the difference between these metric, which gives a measure of the amount of stretching, as the strain tensor, $\epsilon_{ij} \equiv (g_{ij} - \bar{g}_{ij})/2$. In a similar fashion we can define the curvature strain as $\eta_{ij} \equiv (b_{ij} - \bar{b}_{ij})/2$.

The next section discusses the energy cost when the strains are non-zero.

III. ACCOUNTING FOR DYNAMICS

It is well known that the elastic energy of thin shells is composed of a stretching part, which is proportional to the effective elastic thickness, τ, and a bending part, which is proportional to τ^3 [20–22]. Unlike stretching, bending deformations do not stretch the mid-surface of the shell. A quick experiment with paper will convince

you that it costs much less energy to bend a thin sheet than it does to stretch it. Bending energy has also been shown to be negligible in E. *coli* using atomic force microscopy (AFM) studies [23, 24], at least for curvatures much smaller than τ^{-1}. Specifically, we take the elastic energy to be

$$E_{el} = \int d^2u\sqrt{\bar{g}}\; A^{ijk\ell}\left[\frac{\tau}{8}\;\epsilon_{ij}\epsilon_{k\ell} + \frac{\tau^3}{24}\;\eta_{ij}\eta_{ij}\right]. \quad (4)$$

We introduced the isotropic elasticity tensor $A^{ijk\ell} \equiv \lambda\bar{g}^{ij}\bar{g}^{k\ell} + 2\mu\bar{g}^{ik}\bar{g}^{j\ell}$, where λ and 2μ are the Lamé constants, which can be expressed in terms of Young's modulus Y and Poisson's ratio ν as

$$\lambda \equiv \frac{Y\;\nu}{(1+\nu)(1-2\nu)}, \quad \text{and} \quad 2\mu \equiv \frac{Y}{1+\nu}. \quad (5)$$

Due to the τ^3 dependence in the bending energy, the energy cost of deformations with curvature satisfying $\eta_{ij} \ll \tau^{-1}$ will be subdominant. These will correspond to modes with wavelengths larger than τ in Sec. (V).

In these expressions, the growth is implicit: $\bar{g}(t)$ and $\bar{b}(t)$ are assumed to be a slowly-varying function of time. Due to the separation of growth and elastic time scales, we assume the elastic energy is minimized at each instant, with a quasi-static background metric and curvature tensors.

In this paper we give an explicit growth law determining $\partial_t\bar{g}$ in terms of geometry and stress. We could proceed in the same fashion and give a growth law for $\bar{b}(t)$. However, bending energy will be negligible for small curvatures. Furthermore, the exact form of $\bar{b}(t)$ will not be important for curvatures on the order of $\kappa \sim \tau^{-1}$, since for these modes $\bar{b}_{ij} \ll b_{ij}$. Therefore, motivated by simplicity we assume

$$\bar{b}(u^1,u^2,t) = \bar{\kappa}\;\bar{g}(u^1,u^2,t) = \bar{H}\;\bar{g}(u^1,u^2,t). \quad (6)$$

In other words, we assume that the two principle curvatures are the same and are constant in space and time. This assumption avoids introducing model parameters that do not affect the growth of the small curvature modes. However, it is not essential and the analysis of Sec. (V) should go through unchanged if a different growth law is assumed.

In the next section, we will account for the coupling between the target metric and the shape of the shell.

IV. ACCOUNTING FOR GROWTH

In order to have a complete description of a growth process we need to specify how the background metric $\bar{g}_{ij}(t)$ changes with time. A generic class of growth laws can be described by giving the rate of change of the metric as a function of the shape, $\partial_t\bar{g}_{ij}(t) = G_{ij}[\mathbf{X}]$. We will assume that $G_{ij}[\mathbf{X}]$ is a local function of the shape, expressed in terms of the geometrical invariants already introduced. This is consistent with the notion that material insertion is determined from local information only.

There are of course, many possible growth laws consistent with this form; in this section we derive the most general growth law consistent with symmetries. Stated simply, locality is the assumption that the instantaneous change in the metric at a certain position depends only on quantities defined on the surface at that point. Coordinate invariance implies that the instantaneous change in the metric should be a rank-2 tensor on the surface. We assume that this tensor only depends on the local shape (principle of shape dependence) and an applied stress (strain) tensor, which severely restricts the form of the growth law. The constraints on the form of the growth law are coordinate invariance, locality and time homogeneity (absence of explicit time dependence).

We start by describing the geometry dependent terms in the growth law, then we turn to stress-coupled growth.

A. Geometric Coupling

Deriving the geometric growth terms, in the vicinity of some arbitrary point with coordinates $\mathbf{u}$, is most conveniently done by transforming into a coordinate system where the metric at t = 0 is given by the identity matrix $\tilde{g}_{ij} = \delta ij$. More precisely, we can write the metric in the vicinity of a point in Riemann normal coordinates as

$$ds^2 = (du^1)^2 + (du^2)^2 + K(u^1du^2 - u^2du^1)^2 + O(|\mathbf{u}|^3) \quad (7)$$

This requirement however still does not fix the coordinate system. if the principle curvatures satisfy $\kappa_1 \neq \kappa_2$, then the coordinate axes are fixed by requiring the curvature tensor to have the form

$$\tilde{b}_{ij}(\mathbf{u}) = \begin{pmatrix}\kappa_1(\mathbf{u}) & 0\\ 0 & \kappa_2(\mathbf{u})\end{pmatrix} + O(|\mathbf{u}|^2). \quad (8)$$

By locality, we mean that the mechanism responsible for generating the growth only has access to local shape information. To leading order in the vicinity of a point, the shape of the surface is defined by the two principle curvatures[1], and their directions. The principle directions can be taken without loss of generality to be in the u^1 and u^2 directions.

In an infinitesimal time step dt the metric changes by an amount given by

$$\tilde{G}_{ij}(\kappa_1,\kappa_2) = \begin{pmatrix}f_1(\kappa_1,\kappa_2) & f_3(\kappa_1,\kappa_2)\\ f_3(\kappa_1,\kappa_2) & f_2(\kappa_1,\kappa_2)\end{pmatrix}, \quad (9)$$

so that the new metric is $\tilde{g}_{ij} = \delta_{ij} + dt\;\tilde{G}_{ij}$. As mentioned, in this coordinate system $\tilde{G}_{ij}$ can only be a function of κ_1 and κ_2 with no explicit time dependence due to

[1] In other words, the principal curvatures determine the shape of the approximating paraboloid which matches the first two spacial derivatives of the surface.

the assumption of time homogeneity. To anticipate the form of this growth law in a general coordinate system we rewrite it in the form

$$\tilde{G}_{ij} = F_1(\kappa_1,\kappa_2)\ \delta_{ij} + a_0\ F_2(\kappa_1,\kappa_2)\ \tilde{b}_{ij} + F_3(\kappa_1,\kappa_2)\sigma^x_{ij}, \tag{10}$$

where σ^x_{ij} is a Pauli matrix and a_0 is a length scale characterizing the size of the shell. When $\kappa_1 \neq \kappa_2$, the matrices δ_{ij}, $\tilde{b}_{ij}$ and σ^x_{ij} form a complete basis over the space of 2×2 symmetric matrices. In that case, it is possible to express a general choice of the functions (f_1, f_2, f_3) in terms of (F_1, F_2, F_3). However, in the case $\kappa_1 = \kappa_2$ the curvature tensor will also be proportional to the identity matrix. To avoid this problem, we might have replaced $\tilde{b}_{ij}$ with σ^z_{ij} as a basis matrix. However, as we will show next, this is not ideal if the growth process depends purely on the local shape.

When $\kappa_1 = \kappa_2$, it is not possible to uniquely chose coordinate axes at that point because in that case, all directions are equivalent as far as local shape is concerned. Consequently, the growth process cannot favor any direction in this situation. Thus choosing $\tilde{b}_{ij}$ which is proportional to the identity matrix when $\kappa_1 = \kappa_2$ is the proper choice. In addition, since as $u^1 \to -u^1$, $F_3(\kappa_1,\kappa_2) \to -F_3(\kappa_1,\kappa_2)$, the term proportional σ^x_{ij} is seen to violate chiral symmetry. Therefore, in the rest of this paper we will also take $F_3(\kappa_1,\kappa_2) = 0$.

We emphasize that Eq. (10) is only valid for a specific (Riemann normal) coordinate system. We can write it in a general coordinate system by making an arbitrary coordinate transformation. In general, we will have

$$\partial_t \bar{g}_{ij} = F_1(H,K)\ g_{ij} + a_0\ F_2(H,K)\ b_{ij}. \tag{11}$$

Note that we wrote κ_1 and κ_2 in terms of H and K.

We may simplify the growth law by assuming that there is a small length scale λ controlling growth and sensing curvature. In the case of E. *coli*, this length scale is the nanometer scale of proteins as opposed to the $a_0 \sim \mu m$ scale of the bacteria. Compared to the length scale λ, the curvatures can be considered small, which motivates a curvature expansion of the functions

$$F_{(1,2)}(H,K) \approx \alpha_{(1,2)} + \beta_{(1,2)}\ \lambda\ (H-H_0) - \gamma_{(1,2)}\lambda^2\ (K-K_0) + \delta_{(1,2)}\lambda^2\ (H-H_0)^2, \tag{12}$$

where we neglected terms of order λ^3. Note that terms of the form $|\kappa_1 - \kappa_2| = 2\sqrt{H^2-K}$ are possible, but we neglect them due to their non-analyticity. For example, if $\mathbf{X}_S$ describes a sphere, then the rate of growth of a nearby surface $\mathbf{X}_S + \epsilon\ \delta\mathbf{X}$ will scale as $\partial_t g \sim O(\sqrt{\epsilon})$. Assuming an analytic expansion in the pair (H, K) is equivalent to the pair (κ_1,κ_2), unless $H^2 = K$.

Note that we have chosen to expand Eq. (12) to second order in curvature. The reason for this choice, as we will see in Sec. (V), is that the mean curvature and Ricci flow terms are necessary for stability of long wavelength modes. See also Sec. (IV C) for an intuitive explanation of this.

With that in mind, Eqs. (12) and (11) represents the most general geometrically-coupled, purely shape-dependent local growth law expanded up to second order in curvature. Symmetry guarantees that spherical and cylindrical shapes will be fixed points of the evolution as we will show in Sec. V. However, instabilities may lead to spontaneous symmetry breaking and non-symmetric fixed points.

Next we will consider general growth laws in the presence of externally applied disturbances, such as the strain (stress) tensor.

B. Incorporating Stress Coupling

In this section, we seek growth laws that incorporate the role of the strain tensor, defined as $\epsilon_{ij} \equiv (g_{ij} - \bar{g}_{ij})/2$.

We can write all the possible scalars and tensors that are consistent with our criteria. Raising and lowering are done only with g_{ij} and $\epsilon \equiv g^{ij}\epsilon_{ij}$. The different scalars that we can construct are

$$H,\ \epsilon,\ b^{ij}\epsilon_{ij},\ b_{ij}\ b^{ij},\ b^i_k\ b^{ij}\epsilon_{jk}, \bar{\nabla}^i\bar{\nabla}^j\epsilon_{ij},\ \cdots \tag{13}$$

The tensors are

$$\epsilon_{ij},\ g_{ij},\ b_{ij},\ \epsilon^k_i\ b_{kj},\ b^k_i\ b_{kj},\ \bar{\nabla}_i\bar{\nabla}_j\epsilon,\ \bar{\nabla}^k\bar{\nabla}_k\epsilon_{ij}\ \cdots \tag{14}$$

where ∇ and $\bar{\nabla}$ are the covariant derivatives associated with the metrics g_{ij} and $\bar{g}_{ij}$. Terms containing the covariant derivatives will be dropped since they are of order $O(\epsilon\ \lambda^2)$.

We can now construct the most general growth law neglecting terms of order $O(\lambda^3), O(\epsilon^2)$ and $O(\lambda^2\ \epsilon)$. Concretely, we have

$$\begin{aligned}\partial_t\bar{g}_{ij} &= \alpha_1\ g_{ij} + \alpha_2\ b_{ij} + \beta_1\ H\ g_{ij} + \beta_2\ H\ b_{ij} \\ &-\gamma_1\ K\ g_{ij} + \delta_1\ H^2\ g_{ij} + \sigma_1\ \epsilon_{ij} + \sigma_2\ \epsilon\ g_{ij} + \sigma_3\ H\epsilon_{ij} + \\ &\sigma_4\ H\ \epsilon\ g_{ij} + \sigma_5\ \epsilon\ b_{ij} + \sigma_6\ b^{k\ell}\epsilon_{k\ell}\ g_{ij} + \sigma_7\ \epsilon^k_i\ b_{kj}.\end{aligned} \tag{15}$$

In what follows we will neglect terms of order $O(\lambda\ \epsilon)$, which is a reasonable approximation if $H\lambda \gg \epsilon$. This will reduce the number of parameters we have to deal with and will not change our main conclusions (that stress coupling is required to stabilize short wavelength modes and geometric coupling is required for establishing a length scale and stability of the lowest order modes). This approximation leaves only the two leading order stress coupled terms, and removes stress-curvature terms. Furthermore, for linear stability, the δ_1 term will not contribute[2].

Note also that two more terms, coupling growth to the curvature strain η_{ij} and it's trace, are conceivable. However, these terms will scale as curvature coupling terms,

[2] More precisely, the term $\tilde{\delta}_1(H-H_0)^2$ will not contribute to the linearized evolution equations

$\eta_{ij} \sim O(\lambda\ \epsilon)$. Therefore, as described in the previous paragraphs, we will not include these terms in the subsequent analysis.

This leaves seven terms in the growth law, two of which can be fixed by matching to the experimental radius and rate of growth, leaving 5 undetermined constants. Next we will try to gain intuition for the various terms in this growth law.

C. Gaining Intuition For The Growth Law

It is difficult to gain intuition for the terms in the growth law.

The best way to gain intuition is to consider the effect of the various terms on the evolution of special surfaces. Inspired by rod-like E. *coli*, in this paper we focus mainly on elongating cylindrical shapes. However, we will point out how our analysis could be applied to different shapes such as spherical and flat shapes, which are relevant for other interesting growth process as in blooming lilies and rippling leaves [2, 3, 17].

We start with the simplest term, $\alpha_1 g_{ij}$. For very thin surfaces and in the absence of stretching, we can assume that $\bar{g}_{ij} = g_{ij}$. Therefore, with time, the metric will evolve as $g_{ij}(t) = e^{\alpha_1 t} g_{ij}(0)$. Therefore the metric is expanding or contracting exponentially regardless of the initial shape. Furthermore, the linear dimensions of the shell grow exponentially at the rate $R = \alpha_1/2$.

The next term to consider is $a_0\ \alpha_2\ b_{ij}$. This term comes from a simple equation of motion $\partial_t \mathbf{X} = -\alpha_2\ \hat{N}$, which is easy to check with the relation $\partial_t g_{ij} = \partial_t \partial_i \mathbf{X} \cdot \partial_j \mathbf{X} + \partial_i \mathbf{X} \cdot \partial_t \partial_j \mathbf{X}$. This evolution is volume minimizing when α_2 is positive. In the case of cylindrical growth, this term will tend to shrink the radius. In the absence of growth at the end caps, which appears to be approximately true for *E. coli* [13], the length will not be affected by this growth term.

Together, these first two terms give us a way to fix the radius during exponential elongation. Specifically, if we combine these first two terms and set $\alpha_1 = \alpha_2$ we get an exponentially elongating cylinder with fixed radius a_0. The radius of the cylinder that emerges is the one that balances these two terms exactly.

In the case of a growing sphere, setting $\alpha_1 = \alpha_2$ would just stop the growth. On the other hand, the metric of a flat shell would not be affected by this term at all.

Next we consider the term $\beta_1\ (H - H_0)\ g_{ij}$, where we've subtracted $H_0 \equiv -1/(2a_0)$ by changing the definition of α_1. This term couples mean curvature to the rate of growth. It depends on the actual shape and not just on the value of the metric. There is no simple interpretation for $\partial_t \mathbf{X}$ in this case. As we will show, this term with positive β_1 tends to destabilize the radius of the cylinder, as can be seen by solving the equation for a cylinder with radius $a(t) = a_0 + \delta a(t)$. However, we will show in Sec. (V) that this term, with $\beta_1 > 0$, contributes cruicially to the stability of short wavelength modes, particularly in the azimuthal direction.

Intuitively, this can be understood roughly, by looking at the sinusoidal deformations in the azimuthal direction, $a = a_0 + \delta a_0 \sin(m\phi)$, where $m \gg 1$. The mean curvature will be negative in the peaks of this deformation and positive in the troughs, which leads to shrinking of the parts with $a > a_0$ and growth of the parts having $a < a_0$, which in turn leads to a flattening of the pattern.

The α_2 and β_1 terms are dependent on the global orientation of the normal vector $\hat{N}$, which follows from the definition of the curvature tensor. This will not be a problem for the invariance of the growth law if we assume the growth process can distinguish between the inside and the outside of the shell. This is not hard to accept for closed surfaces, as in the case of E. *coli* for example. However, for a growing leaf or flower, it might not be possible to distinguish in from out. Therefore, depending on the details of the process, for growing open shells such as leaves, the terms $\alpha_2 b_{ij}$ and $\beta_1 H g_{ij}$ might be absent due to symmetry considerations.

The term $\beta_2\ (H - H_0)\ b_{ij}$ is related to the mean curvature flow. It would result from the motion $\partial_t \mathbf{X} = -\beta_2\ (H - H_0)\ \hat{N}$ and tends to minimize the area when $\beta_2 > 0$. The stabilizing effect of this term is clear. For a cylinder (or a sphere) with radius $a(t)$, we would get $\dot{a} = 0.5\ a_0^2\ \beta_2\ (1/a - 1/a_0)$. The solution to this equation approaches a_0 as $t \to \infty$, behaving like $a \sim e^{-\beta_2\ t}$. As we will show, stability of long wavelength modes requires $\beta_2 > \beta_1 > 0$ to overcome the destabilizing effect of the β_1 on these modes.

The last geometric growth term we will consider is related to the well known and well studied Ricci flow [25–27]. Namely $\partial_t g_{ij} = -\gamma_1 K g_{ij}$. It is a function of the metric only and we do not need to find the corresponding shape to solve this equation. In order to understand the effect of this term, let's switch to a coordinate system such that the metric can be written in the form $g_{ij} = e^{\rho}\ \delta_{ij}$, this form will be preserved under evolution since the equation can now be expressed as

$$\dot{\rho}\ e^{\rho} = -\frac{\gamma_1}{2}\ e^{\rho}\left(-e^{\rho}\nabla^2\rho\right) \implies \dot{\rho} = \frac{\gamma_1\ e^{-\rho}}{2}\nabla^2\rho. \quad (16)$$

Notice the resemblance of this equation to the diffusion equation. Indeed, in the vicinity of a cylinder we have $\rho \sim 0$, then to leading order this equation becomes exactly the diffusion equation, which tends to wash out the deformations over time, returning the metric back to the constant flat metric. However, note that this equation does not lead to a natural length scale and a cylinder with any radius can be a fixed point of the evolution.

Finally we consider the two stress coupling terms. The term $\sigma_1\ \epsilon_{ij}$ will tend to make the target metric $\bar{g}_{ij}$ evolve towards g_{ij} when $\sigma_1 > 0$. In other words, it makes the surface comply with the applied forces, as in the case of *E. coli* [10].

The term $\sigma_2\ \epsilon$ couples the areal strain to the growth rate, ignoring the shear strain. Coupling to areal strain has been studied in [15] for E. *coli*, and was shown to

lead to stability against bending modes.

Next, we explore how all these terms interact to generate a linearly stable elongating cylinder.

V. LINEAR STABILITY OF ELONGATING CYLINDERS

We now analyze the linear stability of elongating cylindrical shells under the growth law in Eq. (15). As explained below Eq. (15), neglecting the strain curvature terms ($\sigma_i = 0, i > 2$) will not change the main conclusions of this section.

Spherical, planar, and cylindrical symmetries will be preserved under time evolution. Therefore surfaces with these symmetries form a kind of generalized fixed point. We say generalized because they may still be evolving, as in the case of the elongating cylinder. However, instabilities may cause spontaneous symmetry breaking to non-symmetrical shapes. Using linear stability analysis we can determine the parameter values for which a given symmetry is linearly stable.

First, we will establish the importance of coupling to stress by studying the unavoidable instabilities in the purely geometric case. We then show how coupling to stress leads to stability of small wavelength modes and, finally, studying the pure stress coupling case with internal pressure.

A. Purely Geometric Coupling

As mentioned in Sec. IV A, we will ignore terms which have dimensions of inverse length, since these terms will be multiplied by a small length scale λ. The growth law in the purely geometric case is

$$\partial_t \bar{g}_{ij} = \alpha_1\, g_{ij} + \alpha_2\, a_0\, b_{ij} + \beta_1\, a_0\, (H - H_0)\, g_{ij} + a_0^2\, \beta_2\, (H - H_0)\, b_{ij} - a_0^2\, \gamma_1\, (K - K_0)\, g_{ij}. \quad (17)$$

Here the parameters H_0 and K_0 represent some time-independent curvatures, and their definition can be absorbed into $\alpha_{(1,2)}$. We will take them to be the mean and Gaussian curvatures of the fixed point solution. For a sphere with initial radius a_0, we will have $H_0^2 = K_0 = 1/a_0^2$. Naturally for a flat fixed point we would chose $K_0 = H_0 = 0$. Finally, for an elongating cylinder with radius a_0 we will chose $K_0 = 0$ and $H_0 = -1/2a_0$. We've neglected a term proportional to $(H - H_0)^2$ since it will not be important for linear stability.

We start by seeking elongating cylindrical solutions of the form

$$\mathbf{X}_{Cyl} = a\, \hat{s}(\phi) + z\, L(t)\, \hat{z}$$
$$\bar{g}_{ij} = \begin{pmatrix} L_0^2(t) & 0 \\ 0 & a_0^2 \end{pmatrix}, \quad (18)$$

where $\hat{s}$, $\hat{z}$ and $\hat{\phi}$ are the cylindrical basis vectors (see Fig. 2). Here $z \in [0, 1]$ and $L_0(t)$ is the time dependent target length of the shell. The definition of z is convenient because it allows us to consider a boundary value problem on the domain $z \in [0, 1]$ instead of a time dependent domain $[0, L_0(t)]$. Furthermore, note that z and ϕ are thought of as material coordinates. In other words, if a given point on the shell was properly tagged and followed, its trajectory would be given by $\mathbf{X}(z, \phi, t)$, where (z, ϕ) are the coordinates on the initial cylinder at time $t = 0$.

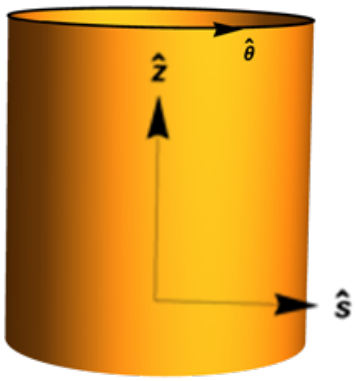

FIG. 2: (Color Online) A coordinate system describing an elongating cylinder. The coordinate z, along the $\hat{z}$ direction, is normalized such that $z \in (0, 1)$.

In order to study the stability of the solution in Eq. (18), we need to first verify that it is a solution of the growth and elastic equilibrium equations in the absence of stress coupling. We assume, for simplicity, $\bar{H} = H_0$, which implies that, for the fixed point solution only (Eq. 18), the perimeter preferred by stretching energy is compatible with the preferred curvature tensor. This assumption is not crucial and can be easily modified, leading to a shifted fixed point radius as in Sec. (V C).

By plugging Eq. (18) into the elastic energy and minimizing with respect to a and L we find, as expected, $a = a_0$ and $L = L_0$. Of course, if $\bar{H} \neq H_0$ or we had nonzero pressure $p \neq 0$, then there will be small corrections to this answer. To find the time dependence of the length, we plug the ansatz Eq. (18) into the geometric growth law Eq. (17). Concretely, we get the conditions

$$\alpha_2 = \alpha_1, \quad \alpha_1 = 2\, R, \quad \text{and} \quad L_0(t) = \ell_0\, e^{R_0\, t}. \quad (19)$$

The first condition results from the requirement of fixed radius. As explained in Sec. (IV C), a fixed radius emerges due to a balancing between isotropic expansion and inward volume contracting growth terms. In other words, if the coefficients of the first and second fundamental forms in the growth law are positive, then the length of the rod that emerges is the length that makes the two terms balance each other. Unlike the cylindrical case, a sphere has two nonzero curved directions, which implies that this balancing would lead to a halting of growth in all direction.

At this point we introduce a perturbation to the elon-

gating cylinder, which has the form

$$\mathbf{X}(z,\phi,t) = a\,[1+\rho(z,\phi,t)]\;\hat{s} + L(t)\,[z+h(z,\phi,t)]\,\hat{z} + a\;\psi(z,\phi,t)\hat{\phi},$$
$$\bar{g}_{ij} = \begin{pmatrix} L_0(t)^2 + G_{zz}(z,\phi,t) & G_{z\phi}(z,\phi,t) \\ G_{z\phi}(z,\phi,t) & a^2 + G_{\phi\phi}(z,\phi,t) \end{pmatrix}. \quad (20)$$

Note that the target metric and target curvature tensors are, in general, no longer compatible after introducing a perturbation to the fixed point solution. Plugging Eq. (20) into the growth equations (17) and assuming the conditions (19) gives us a set of three coupled partial differential equations, which are second order in spacial coordinates and first order in time. However, since we have six unknown function in Eq. (20), we need to use the three elastic equilibrium equations. This is more easily done in Fourier space, which is possible since the equations are linear and the target solution has cylindrical symmetry. Specifically, we have

$$\rho(z,\phi,t) = \sum_m \int \frac{dq}{4\pi^2}\;\rho_{mq}(t)\;e^{im\phi}\;e^{iqz} \quad (21)$$

And similarly for other functions. Periodic boundary conditions in the ϕ direction are implied in this expansion. A more realistic basis in the z direction would be $\sin(n\pi z)$, width $n = 1, 2, \cdots$. However, the expression for the growth rate of perturbations will not depend on this choice as long as we keep in mind that $q_{min} \sim 1/\pi$.

We will solve the equations in two steps. First, we solve the elastic equilibrium equations for the components of $\bar{g}_{ij}$, then we use the growth equations to find the growth rate of radial perturbations $R_\rho(m,q) \equiv \dot{\rho}_{mq}/\rho_{mq}$. The elongating cylinder will be stable if $R_\rho < 0$ for all excitable modes. Since the resulting algebra is too long to show here, we will only show the results in the vanishing thickness ($\tau \to 0$) limit. However the finite thickness results will be plotted and discussed.

We first need to find the elastic equilibrium equations. To leading order, the elastic energy can be written as

$$E_{el} = \sum_{\mathbf{m}} \int \frac{dz\;d\phi\;d^2\mathbf{q}}{4\pi^2} e^{i(m_1-m_2)\phi}\;e^{i(q_1-q_2)z}\;E_{\mathbf{mq}}[\rho_{\mathbf{mq}}, h_{\mathbf{mq}}, \psi_{\mathbf{mq}}] = \sum_m \int dq\;E_{mq}[\rho_{mq}, h_{mq}, \psi_{mq}], \quad (22)$$

where $\mathbf{m} = \{m_1, m_2\}$ and $\mathbf{q} = \{q_1, q_2\}$. We can find the equilibrium equations by taking the derivatives of the energy with respect to the independent variable. Specifically

$$\frac{\delta E_{mq}}{\rho_{mq}} = \frac{\delta E_{mq}}{h_{mq}} = \frac{\delta E_{mq}}{\psi_{mq}}. \quad (23)$$

for vanishing thickness ($\tau \to 0$), the solution to Eq. (23) is given by

$$\rho_{mq} = \frac{m^2\;G_{zz} - 2\;m\;q\;G_{z\phi} + q^2\;G_{\phi\phi}}{2\;a_0\;q^2},$$
$$h_{qm} = -\frac{i\;G_{zz}}{2\;q\;L_0^2} \quad \text{and}$$
$$\psi_{mq} = i\frac{m\;G_{zz} - 2\;q\;G_{z\phi}}{2\;a_0^2\;q^2}, \quad (24)$$

which is an isometry of the metric given in Eq. (20). The analogous expression in the finite thickness case ($\tau \ll 1$) is too long and uninformative to show here.

We can invert Eq. (24) to eliminate the components of $\bar{g}_{ij}$ from the growth equations. After plugging the resulting answer in the growth law, we obtain three first order ODEs for the functions $\rho_{mq}(t)$, $h_{mq}(t)$ and $\psi_{mq}(t)$. For the zero thickness case, $\tau \to 0$, the growth equations become

$$\frac{\dot{\rho}_{mq}}{\rho_{mq}} = -\frac{1}{4}\left(\Gamma_1 + q_P^2\;\Gamma_2 + m^2\;\Gamma_3 + \frac{m^2(m^2-1)\Gamma_4}{q_P^2}\right),$$
$$\dot{h}_{mq}(t) = -\frac{im}{4}\left(\Gamma_5 + \frac{(m^2-1)\;\Gamma_4}{q_P^2}\right)\rho_{mq}(t) \quad \text{and}$$
$$\dot{\psi}_{mq}(t) = -\frac{im}{4}\left(\Gamma_5 + \frac{(m^2-1)\;\Gamma_4}{q_P^2}\right)\rho_{mq}(t), \quad (25)$$

were we introduced the physical wavenumber as $q_P \equiv a_0\;q/L_0(t)$. With this definition, the instantaneous wavelength of the deformation is $\lambda_P = a_0(2\pi/q_P)$. It is interesting to note that even though q is time independent, q_P is not. This is due to the stretching of the wavelengths during elongation. We have also introduced the (q_P, m) independent rates Γ_i, which are given by

$$\Gamma_1 = \beta_2 - \beta_1 - 4R_0,\;\; \Gamma_2 = 2\gamma_1 + \beta_1 - \beta_2,$$
$$\Gamma_3 = 2\;\gamma_1 + 2\;\beta_1 - \beta_2, \Gamma_4 = \;\beta_1$$
$$\text{and}\;\; \Gamma_5 = 2\gamma_1 + \beta_1 - 4R_0. \quad (26)$$

Note that h_{mq} and ψ_{mq} satisfy the same equation and they both approach a constant value when $\rho_{mq} \to 0$.

It turns out, this last fact is true for any coordinate invariant growth law. This is easy to see by considering Eq. (20) with $\rho, \psi, \dot{h} \to 0$, for which the surface becomes $\mathbf{X} = a_0\;\hat{s} + L(t)(z + h_0(z,\phi))$. It can be shown that this surface is a cylinder for an arbitrary function $h_0(z,\phi)$. In

other words, this deformation is equivalent to a coordinate transformation. Since the growth law is coordinate independent, a deformation with arbitrary $h_0(z,\phi)$ is a fixed point solution, which, just as Eq. (18), describes an elongating cylinder. This explains why $\dot{h}_{mq}=0$ when $\rho_{mq}=0$. A similar argument can be given for ψ_{mq} in the linear regime.

Thus, a sufficient and necessary condition for linear stability is $\rho_{mq}(t\to 0)=0$, or that $R_\rho \equiv \dot{\rho}_{mq}/\rho_{mq}<0$ for all permissible wavenumbers q_P and m. However, there is a subtlety associated with this stability condition.

As mentioned above, q_P is time dependent and as the wavelength of a solution is stretched, its rate of growth will also change. In particular, it is conceivable that $R_\rho>0$ for a given q_P, but the solution is still stable. This is because the solution only experiences this instability for a short period of time before the physical wavelength q_P changes to a value where $R_\rho<0$. Keep in mind however, that this only happens if $R_\rho>0$ for a small range of q_P, at the onset of an instability. In addition, some long wavelength instabilities might not be realized until the shell length $L_0(t)$ reaches a certain value.

Keeping all of that in mind, we derive the necessary condition for stability of all modes as $t\to\infty$, which implies $R_\rho<0$ for all q_P and m up to a high cutoff.

From Eq. (25) we find the rate of growth to be

$$R_\rho = -\frac{1}{4}\left(\Gamma_1 + q_P^2\,\Gamma_2 + m^2\,\Gamma_3 + \frac{m^2(m^2-1)\Gamma_4}{q_P^2}\right). \quad (27)$$

A more complicated expression also exists in the finite thickness regime which, interestingly, also depends only on the combinations Γ_i. Apart from the growth law parameters, R_ρ depends only on the physical wavelengths in units of a_0. The wavenumber m can in principle be any integer, however there will be a high cutoff value corresponding to a small length scale. q_P on the other hand will have a lower bound as well, corresponding to the finite size $L_0(t)$. Interestingly, this lower bound is time dependent, decreasing with time. To zeroth order, we will require stability for all m and all q_P without bounds.

We first find the stability region in parameter space for the zero thickness case. Then we will see how finite thickness changes the situation. It is clear from Eq. (27) that we must have $\Gamma_1,\Gamma_2,\Gamma_3,\Gamma_4>0$. This leads to the conditions

$$\beta_1>0,\quad \beta_2>4R_0+\beta_1,\quad 2\gamma_1>\beta_2-\beta_1 \quad (28)$$

We've already anticipated these relations in Sec. (IV C). Recall that the β_2 (mean curvature flow) term stabilizes long wavelengths and β_1 and γ_1 contribute to stability of shorter wavelengths, thus explaining these relations. It is one of the main conclusions of this paper that the mean curvature flow is important for the stability of the longest wavelength modes.

The relations in Eq. (28) define three planes that bound the stability region in parameter space. Fig. (3) shows a cross section of this region along with modes

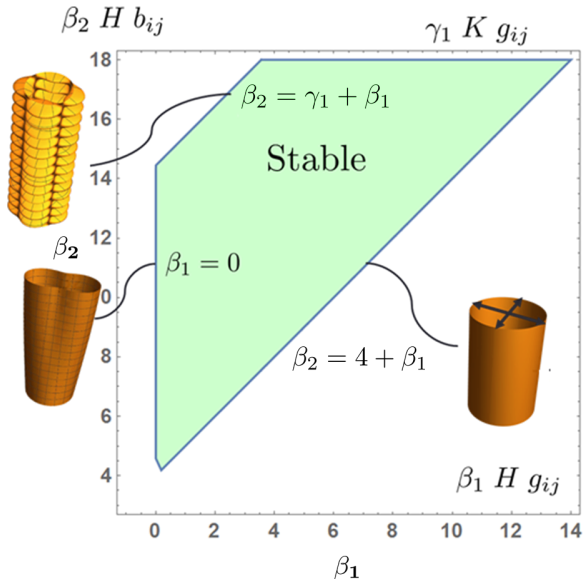

FIG. 3: (Color Online) This figure shows the stability region in the (β_1,β_2) plane with $\gamma_1=15$ and stress coupling $\sigma_1=\sigma_2=20$. Here and in all plots $R_0=1$, $a_0=1$, $\nu=1/3$, $\eta_B=0.01^3$ and $\eta_S=0.01$. We also show the nature of the instabilities when crossing the different boundaries. The nature of these instabilities depends on $\sigma_1,\sigma_2,\eta_B>0$, however the region itself would look the same in the case $\sigma_1,\sigma_2,\eta_B=0$.

of instability when $\sigma_1,\sigma_2,\tau>0$, which will be discussed shortly. In fact, this is also the region of stability for the finite thickness and stress coupling cases.

Now we turn to the interesting question of what happens near the three boundary surfaces of the stability region. Consider approaching the boundary $\Gamma_1=0$, while $\Gamma_2,\Gamma_3,\Gamma_4>0$. It is easy in this case, to see that the rate is maximized when $m=0$ and $q_P\to 0$. This is illustrated in Fig. (4). As we saw in Sec. (IV C), the $\beta_1>0$ term destabilizes the long wavelength modes if β_2 is not large enough.

It can also be seen readily from Eq. (27) that crossing the boundary $\beta_1=0$ results in modes with high $m\sim m_{cutoff}$ and small $q_P\sim a_0\pi/L_0$ dominating the shape. Which confirms out intuition that $\beta_1 H g_{ij}$ stabilizes large m modes (Sec. IV C). Here m_{cutoff} is the mode number at which our long wavelength approximation fails. In fact, finite thickness regularizes this behavior. As can be seen from Fig. (5) the instability in the finite thickness case happens at $m=2$ and $q_P\sim 0.2$.

We may also get an instability that favors modes of high $q_P\sim q_{cutoff}$ by setting $\Gamma_2<0$. Unfortunately in this case, the bending energy does not regularize the behavior at large q, and in fact, seems to make these modes more unstable. In particular, in the finite thickness case we have

$$\lim_{q_P\to\infty} R_{\rho B} = -\lim_{q_P\to 0} R_{\rho B} = -\lim_{m\to\infty} R_{\rho B} = 4\,R, \quad (29)$$

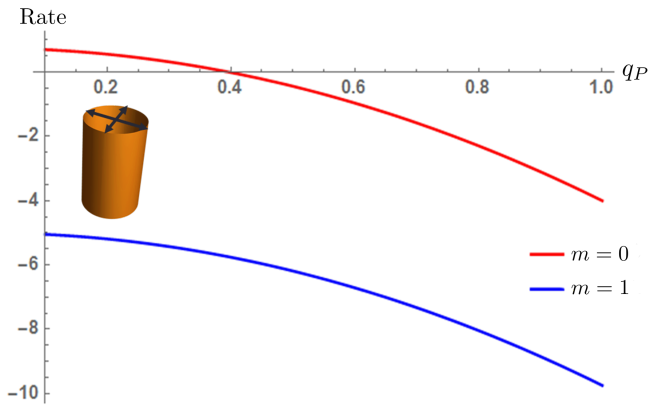

FIG. 4: (Color Online) This figure shows the growth rate as function of q_P for different values of m when $\beta_2 < \beta_1 + 4R_0$. Note that the maximum rate happens at $m = 0$ and $q \sim 0$.

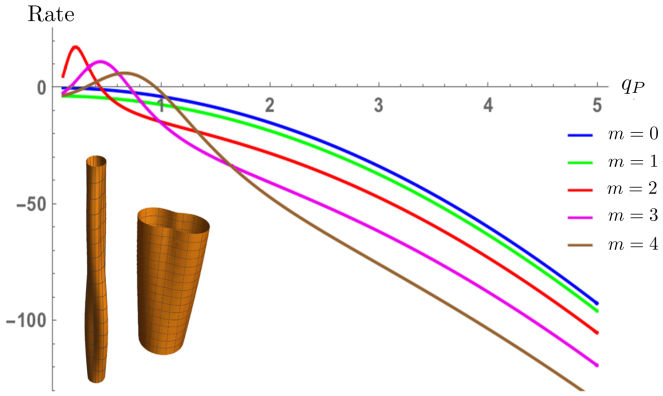

FIG. 5: (Color Online) This figure shows the growth rate as function of q_P for different values of m when $\beta_1 < 0$. Note that the maximum rate happens at $m = 2$.

where the index B in $R_{\rho B}$ is added to emphasize that bending energy is considered. We see from Eq. (29) that the effect of bending energy is to make the high m modes always stable, while high q_P modes are unstable for all parameter values (see Fig. 6). This non-intuitive result is one of the main contributions of this paper.

The reason this is counter intuitive is because bending is expected to suppress modes of small wavelength rather than enhance them, which is true in the static setting. In a growing shell, to suppress the small wavelength fluctuations, their growth in the target metric must be suppressed. In the absence of bending, this suppression happens through the Γ_2 term in Eq. (27). As we show in the appendix, bending suppresses this term indirectly by inhibiting high curvature modes. Amazingly, by suppressing high curvature modes, you allow them to grow further in the target metric (see appendix).

Regardless of the source of these instabilities, a growing shell – such as E. *coli* – must find a way to avoid these instabilities. One possibility is that the small wavelength cutoff, λ, is on the order of the thickness of the shell. This

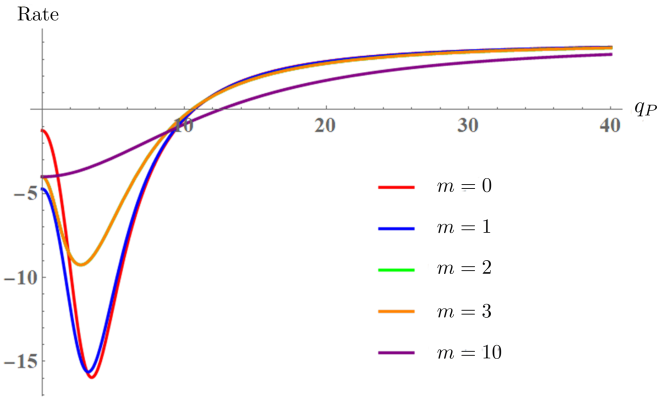

FIG. 6: (Color Online) This figure shows that all modes are unstable in the absence of stress coupling for high values of $q_P > a_0/\tau$. Here we set $\eta_S^3 = \eta_B = 0.3^3$, $\beta_1 = 5$, $\beta_2 = 14$, $\gamma_1 = 9$, $\sigma_{1,2} = 0$ and $\nu = 1/3$. Fig. 8 shows how stress coupling modifies and stabilizes this behavior.

is a reasonable possibility since the expansion of the energy in powers of thickness breaks down. For wavelengths that are close to the thickness, the rate behaves as

$$R_{\rho B}(q_P \to \frac{a_0}{\tau}) = -4\,\frac{\Gamma_2 - R_0\,(1-\nu^2)}{1-\nu^2}. \tag{30}$$

Therefore, in the absence of stress coupling we must require that $\Gamma_2 > R_0\ (1-\nu^2)$ and $q_P \lesssim \tau$ to achieve stability. The appearance of the material parameter ν (Poisson's ratio) in this expression is due to its effect on the response of the shape to the bending force, which in turn affects the growth rate.

Another, more robust way to stabilize small wavelength fluctuations is accomplished by coupling growth to stress, which we turn to next.

B. Stress Coupling To The Rescue

As we have seen in Sec. (IV C), the term $\sigma_1\ \epsilon_{ij}$ with $\sigma_1 > 0$ tends to make the target metric grow to comply with the applied force. So if the applied force is bending, then we may expect that adding stress coupling can lead to suppression of the modes $q_P \gtrsim \tau$. After ignoring terms of order $O(\lambda\,\epsilon)$ as described before, we step through the calculation in a similar manner to that described above. We eventually get

$$\lim_{q\to\infty} R_{\rho B} = 4\,R_0 - \frac{1}{2}\left(\sigma_1 + \frac{1-2\nu}{1-\nu}\sigma_2\right). \tag{31}$$

In other words, if the stress coupling is strong enough, then small wavelength modes are always stable no matter what parameters you use. It can also be shown, for small enough thickness, that the stability region in this case is the same as before (Figs. 3 and 7). In addition, the $\beta_1 < 0$ and $\beta_2 < \beta + 4\ R$ instabilities still look the same (see Figs. 4 and 5). However, as Fig. (8) shows,

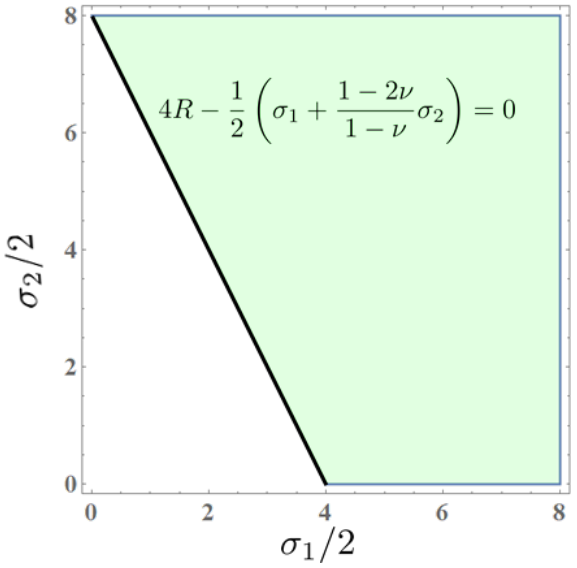

FIG. 7: (Color Online) This figure shows the stability region in the (σ_1, σ_2) plane with $\gamma_1 = 15$, $\beta_1 = 6$ and $\beta_2 = 16$. Here and in all plots $R_0 = 1$, $a_0 = 1$, $\nu = 1/3$, $\eta_B = 0.01$[3] and $\eta_S = 0.01$.

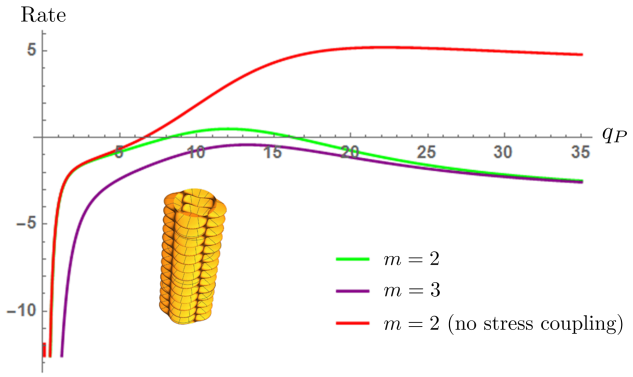

FIG. 8: (Color Online) This figure shows the growth rate as function of q_P for different values of m when $\Gamma_2 < R_0\,(1-\nu^2)$ and $\sigma_1, \sigma_2 > 8R$. Note that the maximum rate happens at $m = 2$ and at a finite value of $q_P \sim O(10)$. For comparison, we have also included a plot of the rate in the absence of stress coupling.

when we cross the $\Gamma_2 = R_0\,(1-\nu^2)$ plane, the instability will not start at the highest q_P modes as before. In fact, it will happen typically for $m = 2$ and $q_P \sim O(10)$.

Thus, stress coupling enhances the stability against small wavelength deformations. And so, having both geometric and stress couplings can lead to stability of an elongating cylinder against all modes for a broad range of parameters.

Next, we turn to the possibility of stability with stress coupling alone.

C. (Almost) Purely Stress Coupling

As we have seen, coupling to stress has a stabilizing effect on short wavelength modes. Therefore, it is natural to consider a class of growth laws that only couples to stress. Such growth can happen, for example, if the rate of insertion is affected by the size of the exposed pores on a surface (see the appendix for an example).

The first thing we note is that the stress-coupled growth terms in Eq. (15), α_1, σ_1 and σ_2 do not lead to a natural length scale as in the case of curvature coupling. Furthermore, a cylinder elongating in only one direction implies an asymmetry in the material properties. In other words, there must be a template to guide the growth to achieve an elongating cylindrical solution.

For these reasons, we retain the leading order curvature term $\alpha_2 b_{ij}$. In other words, growth can distinguish the two principal directions. Another manifestation of these issues is that stress coupled growth will have difficulties in stabilizing the largest wavelength modes.

To make this discussion more interesting, and perhaps to be more relevant to the problem of rod-like E. *coli*, we will include a pressure like force $\mathbf{F}_P = p_0 \hat{N}$. We say pressure like since this force acts on the surface of the cylinder and not the end caps. Since we are interested in the long wavelength behavior, we will neglect the bending forces. In addition, we will assume Poisson's ratio to be zero, $\nu = 0$[3].

We can now follow the analysis starting with Eq. (18). Unlike previously, $a \neq a_0$ due to pressure. In fact, we will have, for the fixed point solution, that

$$a = a_0(1 + \delta a), \qquad \delta a \sim \frac{p_0\, a_0}{\tau\, Y}. \tag{32}$$

For example, E. *coli*, will have $\delta a \sim O(0.05)$.

Next, we can follow the strategy outlined previously to obtain the rate of growth, R_ρ of various modes q_P and m to leading order in δa (linear elasticity). We show here the results for the longest wavelength modes since we expect them to be the problematic modes in the case of stress coupling. Specifically, as $q_P \to 0$, we get

$$\begin{aligned} R_\rho(m=0) &\approx R + (3R + \sigma_1 + \sigma_2)\, O(\delta a) \\ R_\rho(m=1) &\approx \frac{(6R + \sigma_1 + \sigma_2)\, O(\delta a)}{2q_P^2} \\ R_\rho(m=2) &\approx -\frac{(10R + \sigma_1 + \sigma_2)\, O(1)}{2q_P^4}. \end{aligned} \tag{33}$$

These modes cannot be stabilized simultaneously. We have already seen that for small wavelength modes, we need $\sigma_1 + \sigma_2 > 8R > 0$ for stability. Therefore in the stress coupled case the long wavelength modes are harder to stabilize. Out of the terms we considered, only the

[3] These assumptions are to simplify the discussion and can be modified depending on the application

mean curvature flow term, $\beta_2(H - H_0)g_{ij}$, can stabilize the $(m = 0, q \to 0)$ mode. This might be a reason why both stress coupling and geometric coupling have been observed in E. *coli* [13–15, 32].

VI. CONCLUSION

Growing elastic shells appear in a wide variety of contexts ranging from synthetic and natural shape changing materials that can be activated by spatially controlled swelling [7–9] all the way to the growth of biomaterial sheets and planar tissues by the addition of material and proliferation of cells respectively [3, 4, 11]. In this paper, we have addressed for the first time, the dynamics of such growing sheets and the consequences for their stability. We have assumed that a growing shell, to which material is being added and removed, can be described with a slowly changing target metric. This is because, as a shell's structure rearranges, the natural distances between points in the shell change. Within this setup there are many ways that the metric can change with time. It can change in a prescribed shape-independent way, as done in experiments like [7, 9], it can be coupled to an externally applied field like a stress tensor or an ordered template [14] or it can be dependent purely on shape as in Eq. (11).

Regulation of such growth to yield a desired structure typically requires a control mechanism. Such control mechanisms could couple the processes driving the growth to global properties of the shape, or to local properties of the shape, allowing the material to act locally and think globally. Therefore, in this paper we explored the coupling of the change in the metric to local properties of the sheet - the local shape, and a stress tensor. Symmetry and locality arguments help reduce the space of possible metric changes down to the form given in Eq. (15).

After constructing this general growth law, as a first step, we analyzed the linear stability of an elongating cylinder under purely geometric coupling (Sec. V A). Surprisingly, we found that for any choice of model parameters, modes with wavelengths on the order of the thickness ($q_P \sim 1/\tau$) cannot be stabilized (see Figs. 6,7). This unexpected result means that a growth law that is only shape-dependent cannot lead to an elongating cylinder that is linearly stable to small wavelength fluctuations.

Since biological systems appear to be able to solve this problem, we consider two possibilities. First, there might be a cutoff beyond which the assumptions under which our growth law is derived will not be valid. One could imagine, for example, that nonlinearities might result in the suppression of instabilities. However, even in such cases, one might expect to see the vestiges of the onset of the instability. This raises the intriguing possibility that such arrested instabilities could be used to create small scale patterns.

To more robustly stabilize the growth, we consider a second mechanism, stress coupling, discussed in Sec. (V B). In particular when the effects of stress coupling are included we find that these small wavelength modes become universally stable, as shown in Figs. (8 and 7). This is because the stress coupling terms tend to make the target metric grow in a viscoelastic-like way to conform with the applied forces as discussed in Sec. IV C. In this situation, the applied forces are the bending forces (in E. *coli*, turgor pressure contributes as well), and since small wavelength modes contribute a lot of bending energy they will be suppressed. Note that both the applied force and the stress coupling contribute to this result.

Interestingly, it was shown in [15] that coupling to areal strain alone can result in straightening of a bent rod. However, under this growth law a shell might still be unstable with respect to different modes of deformation. Experiments involving controlled perturbations of the growth laws can yield a significant amount of information on the exact nature of the couplings. To this end, we are currently working on fitting the parameters of the model to experiments where bacteria are subjected to bending forces and oscillatory osmotic shocks resulting in perturbations in localization and dynamics of growth [14, 28]. One could also imagine directly probing the instabilities by growing E. *coli* in confining geometries with shapes of a specific wavelength in the z and ϕ directions. The exact form of R_ρ could then be compared to the results of the experiment.

Finally, it is also conceivable that a certain shape cannot be stabilized at all, just as we've seen that, with purely geometric coupling, an elongating cylindrical shell would always be unstable to small wavelength fluctuations. While flat, cylindrical and spherical shapes are fixed points of the growth law due to symmetry, an interesting project would be a characterization of all the possible stable shapes within this framework and relating them to the kinds of patterns observed in nature.

VII. ACKNOWLEDGMENT

We acknowledge useful and enlightening conversations with B. Chen, L. Mahadevan, A. Amir and K.C. Huang. CS and SA were funded by the National Science Foundation under award DMR-1507377 and AG was partially supported by National Science Foundation NSF grant DMS-1616926, a James S. McDonnell Foundation Award and in part by the NSF-CREST: Center for Cellular and Bio-molecular Machines at UC Merced (NSF-HRD-1547848).

VIII. CONFLICT OF INTEREST

There are no conflicts of interest to declare

[1] Thompson, D. W. (1917). On Growth and Form, 1st edn. Cambridge, UK: Cambridge University Press.
[2] M. Marder, E. Sharon, S. Smith and B. Roman. *Theory of edges of leaves.* **62**, 4. (2014)
[3] H. Liang, L. Mahadevan. *Growth, geometry, and mechanics of a blooming lily*, Proc. Natl. Acad. Sci. USA **108**, 5516-5521 (2011).
[4] Dervaux, J. and Amar, M.B., "Morphogenesis of growing soft tissues," Phys. Rev. Lett. **101**, 068101 (2008).
[5] Tallinen T, Chung J., Rousseau F , Girard N, Lefvre J and Mahadevan L. *On the growth and form of cortical convolutions.* **12**, 588-593. (2016).
[6] Castle, T., Cho, Y., Gong, X., Jung, E., Sussman, D.M., Yang, S. and Kamien, R.D., 2014. Making the cut: Lattice kirigami rules. Physical review letters, 113(24), p.245502.
[7] Y. Klein, E. Efrati and E. Sharon. *Shaping of elastic sheets by prescription of non-Euclidean metrics.* Science **315**, 1116-1120 (2007).
[8] Efi Efrati; Eran Sharon; Raz Kupferman. *The metric description of elasticity in residually stressed soft materials.* Soft Matter. **9**:(34)8187-8197. (2013)
[9] Kim J, Hanna JA, Byun M, Santangelo CD, Hayward RC. "Designing responsive buckled surfaces by halftone gel lithography," Science **335**, 1201-1205. (2012).
[10] Amir A., Teeffelen S. *Getting into shape: How do rod-like bacteria control their geometry?* Syst Synth Biol. **8(3)** , 227-235. (2014).
[11] Chang F, Huang KC. *How and why cells grow as rods.* BMC Biol. **12**, 54. (2014).
[12] D. Scheffers and Mariana G. Pinho. *Bacterial Cell Wall Synthesis: New Insights from Localization Studies.* **69(4)**, 585-607. (2005).
[13] T. Ursella, J. Nguyenb , R. D. Mondsa, A. Colavinc, G. Billingsd, N. Ouzounove, Z. Gitaie, J. W. Shaevitzb and K. C. Huang. *Rod-like bacterial shape is maintained by feedback between cell curvature and cytoskeletal localization.* PNAS. **111(11)**, E1025-E1034. (2014).
[14] Amir A, Babaeipour F, McIntosh D, Nelson D, and Jun S. *Bending forces plastically deform growing bacterial cell walls.* PNAS. **111**, 57785783. (2014).
[15] Wong F, Renner LD, zbaykal G, Paulose J, Weibel DB, van Teeffelen S, Amir A. *Mechanical strain sensing implicated in cell shape recovery in Escherichia coli*, Nature Microbiology. **2**, 17115 (2017)
[16] Shraiman, B. I. (2005) Proc. Natl. Acad. Sci. USA **102**, 33183323
[17] J. Pulwicki, *Dynamics of Plant Growth; A Theory Based on Riemannian Geometry*, **arXiv:1602.01778**, (2016)
[18] M.P. Do Carmo, *Differential Geometry of Curves and Surfaces* (Prentice-Hall, 1976).
[19] R.M. Wald , *General Relativity* (University of Chicago Press, 1984).
[20] Augustus Love. *A treatise on the mathematical theory of elasticity.* 1, (1892). <hal-01307751>
[21] P. Audoly and Y. Pomeau, Elasticity and Geometry (Oxford University Press, Oxford, 2010).
[22] L.D. Landau and E.M. Lifshitz, Theory of Elasticity (Butterworth-Heinemann, Oxford, 1986).
[23] M. Arnoldi, M. Fritz, E. Bauerlein, M. Radmacher, E. Sackmann, and A. Boulbitch, Phys. Rev. E 62, 1034 (2000).
[24] Y. Deng, M. Sun, & J. W. Shaevitz, *Direct measurement of cell wall stress stiffening and turgor pressure in live bacterial cells.* Phys. Rev. Lett. **107**, 158101 (2011).
[25] R Hamilton, J Diff Geom 17 (1982) 255
[26] O. C. Schnurer, F. Schulze, and M. Simon, *Stability of Euclidean Space Under Ricci Flow*, **arXiv:0706.0421**, (2008)
[27] J. Cortissoz, A. Murcia, *The Ricci flow on a cylinder*, **arXiv:1604.02132**
[28] ER Rojas, JA Theriot, KC Huang, *Response of Escherichia coli growth rate to osmotic shock,* PNAS **111** 7807-7812 (2014).
[29] D. A. Quint, A. Gopinathan, and Gregory M. Grason. *Shape Selection of Surface-Bound Helical Filaments: Biopolymers on Curved Membranes.* Biophys. J. **111(7)** 1575-1585. (2016).
[30] Wang, Siyuan et al. *Cell Shape Can Mediate the Spatial Organization of the Bacterial Cytoskeleton.* Biophys. J. **104(3)**, 541-552 (2012)
[31] Y. Fily, A. Baskaran, M. F. Hagan. Active Particles on Curved Surfaces. arXiv:1601.00324 [cond-mat.soft].
[32] Hussain S, Wivagg CN, Szwedziak P, Wong F, Schaefer K, Izore T, Renner LD, Sun Y, Bisson Filho AW, Walker S, et al. *MreB Filaments Create Rod Shape By Aligning Along Principal Membrane Curvature.* [Internet]. 2017.

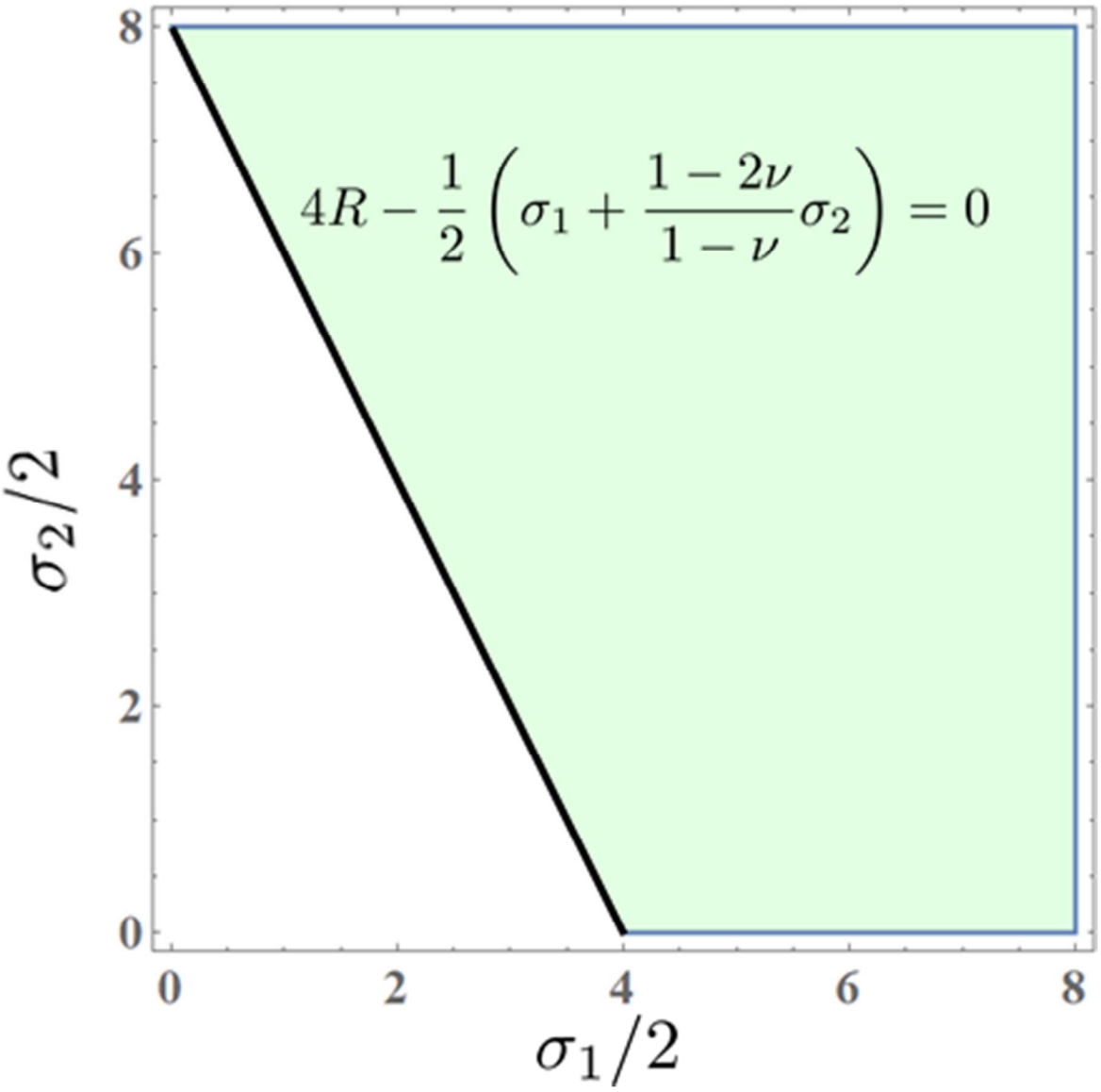
$4R - \frac{1}{2}\left(\sigma_1 + \frac{1-2\nu}{1-\nu}\sigma_2\right) = 0$
8
6
4
2
0
0
2
4
6
8
$\sigma_2/2$
$\sigma_1/2$

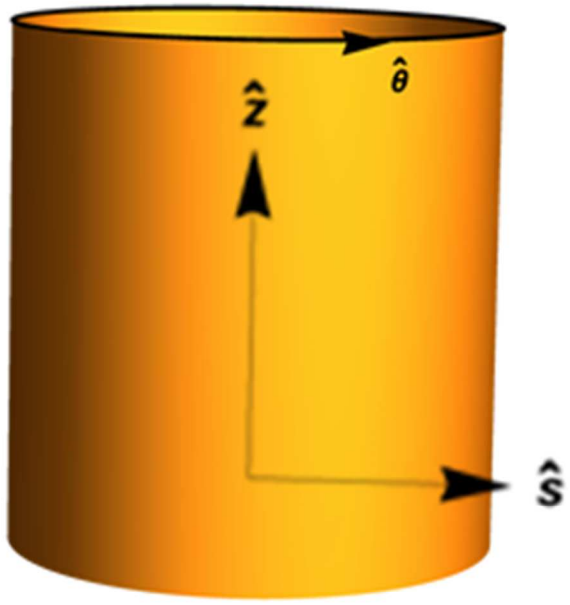
$\hat{\theta}$
$\hat{z}$
$\hat{s}$

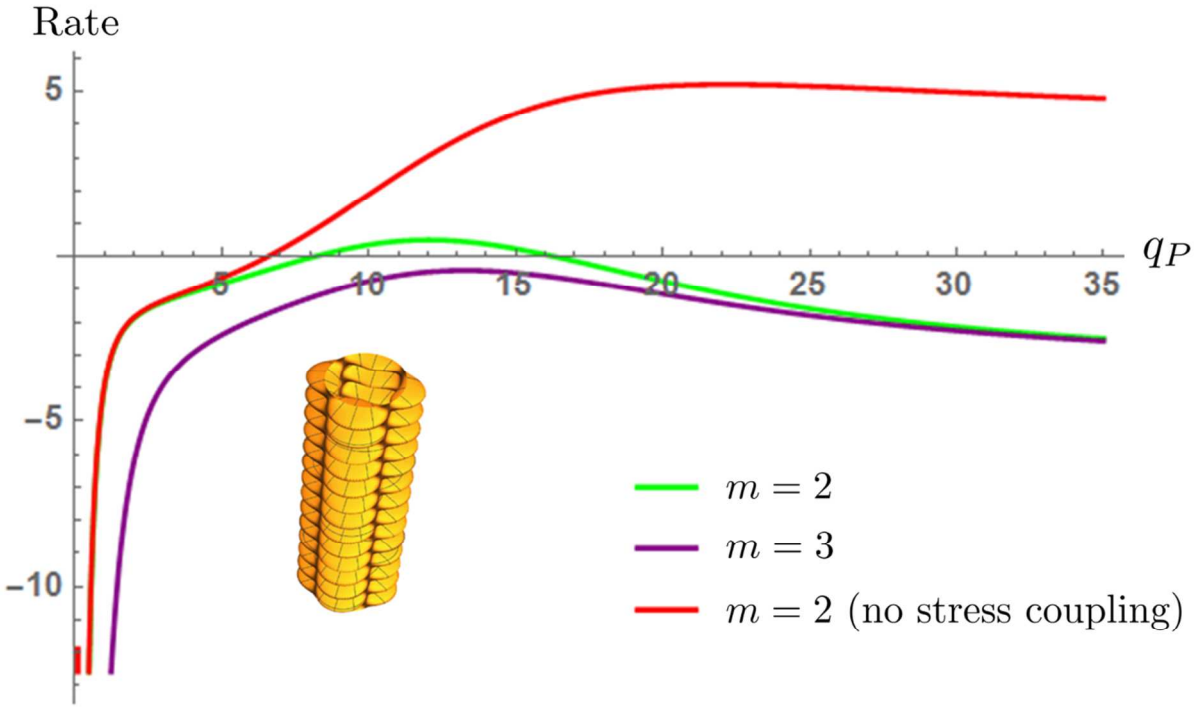
Rate
5
−5
−10
5
10
15
20
25
30
35
q_P
$m = 2$
$m = 3$
$m = 2$ (no stress coupling)

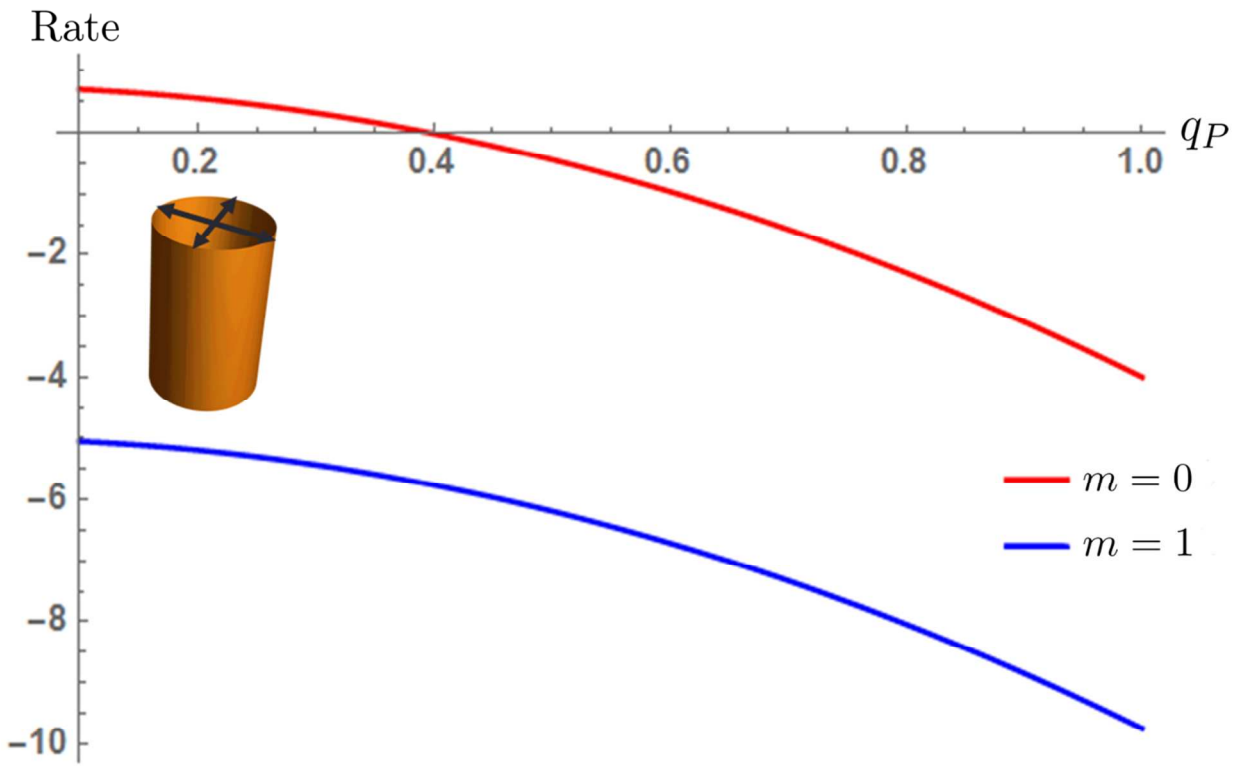
Rate
q_P
0.2
0.4
0.6
0.8
1.0
−2
−4
−6
−8
−10
$m = 0$
$m = 1$

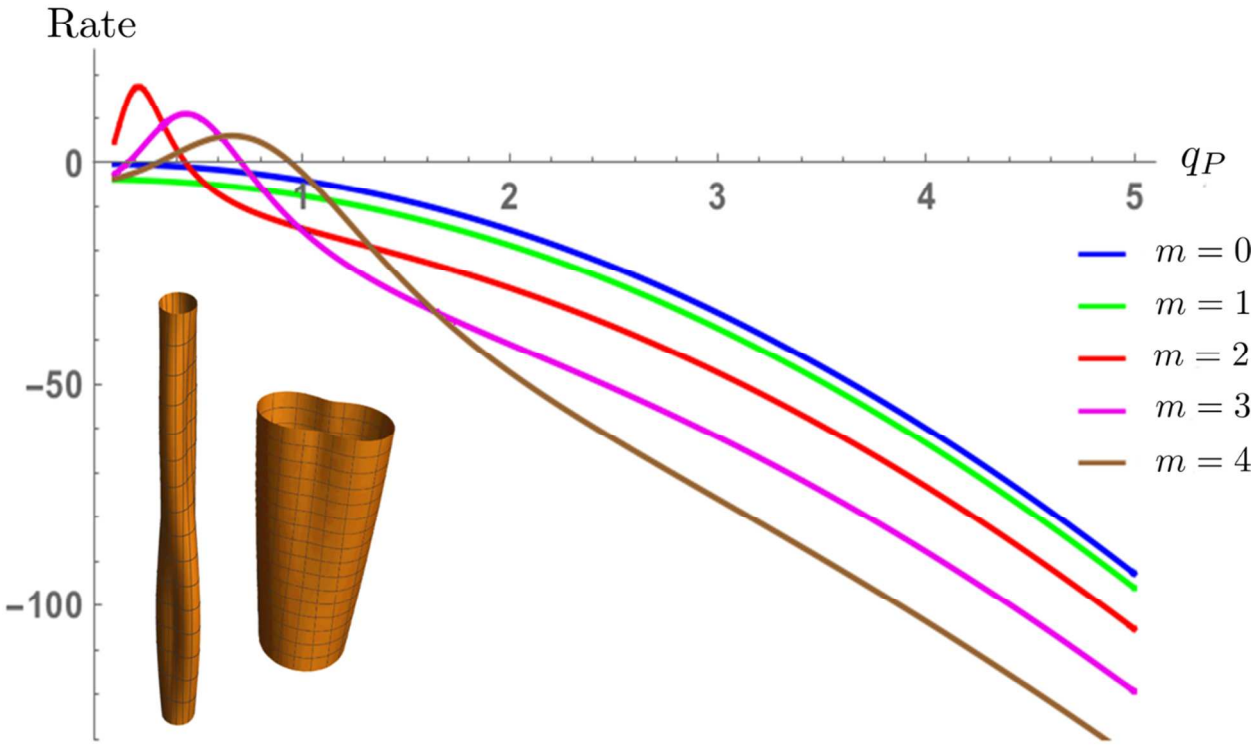
Rate
q_P
0
1
2
3
4
5
−50
−100
$m = 0$
$m = 1$
$m = 2$
$m = 3$
$m = 4$

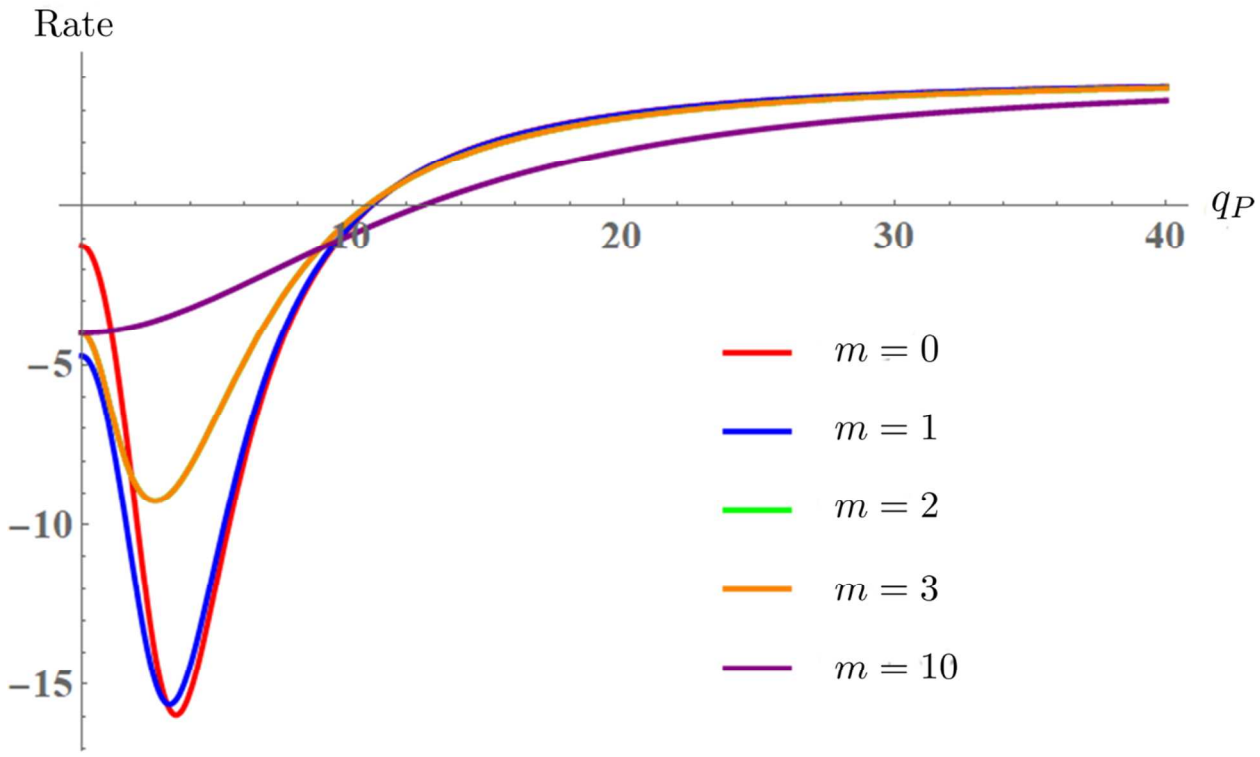
Rate
q_P
10
20
30
40
−5
−10
−15
$m = 0$
$m = 1$
$m = 2$
$m = 3$
$m = 10$

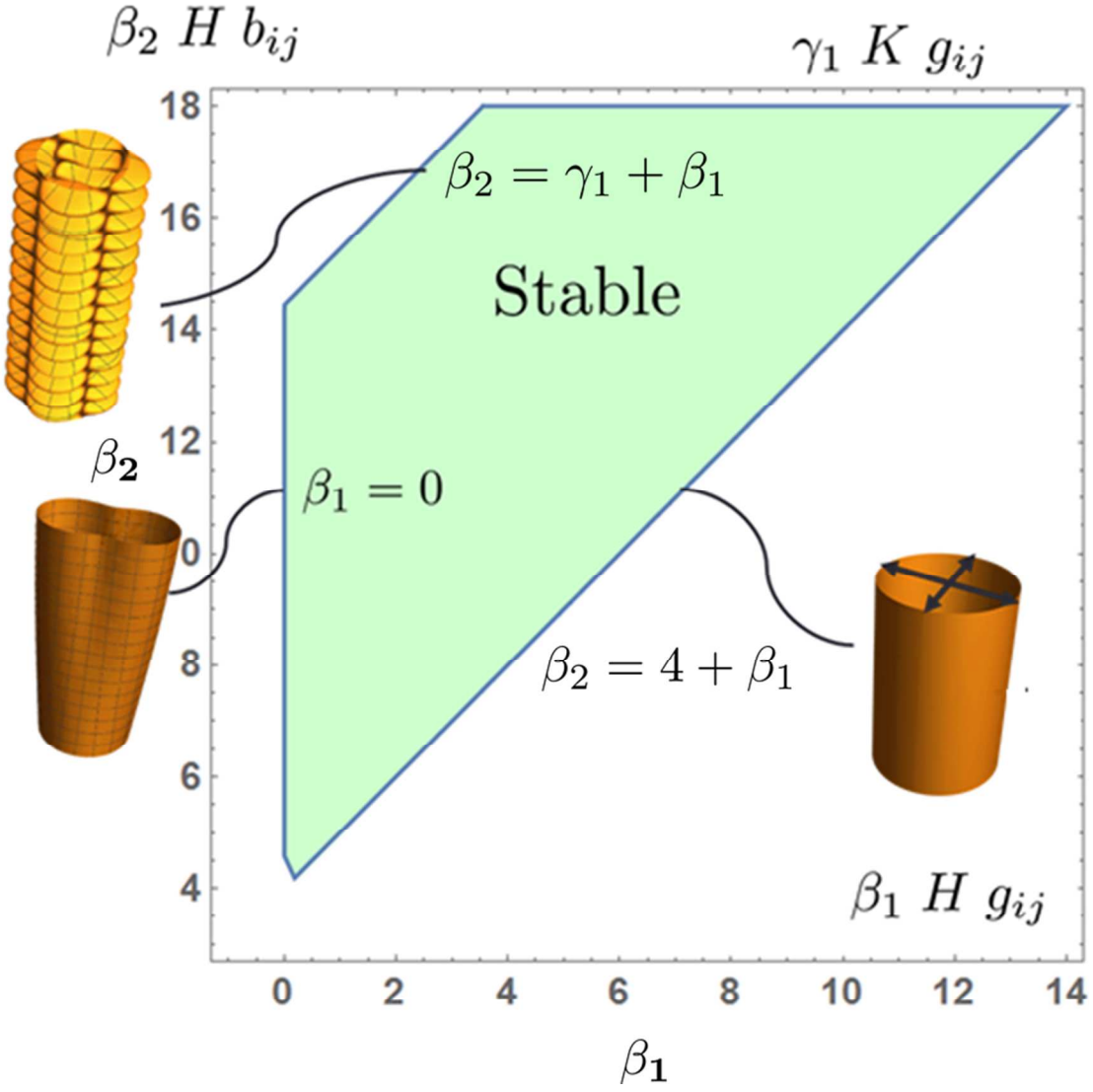
$\beta_2\ H\ b_{ij}$
$\gamma_1\ K\ g_{ij}$
$\beta_2 = \gamma_1 + \beta_1$
Stable
$\beta_1 = 0$
$\beta_2 = 4 + \beta_1$
$\beta_1\ H\ g_{ij}$
β_2
β_1
18
16
14
12
0
8
6
4
0
2
4
6
8
10
12
14

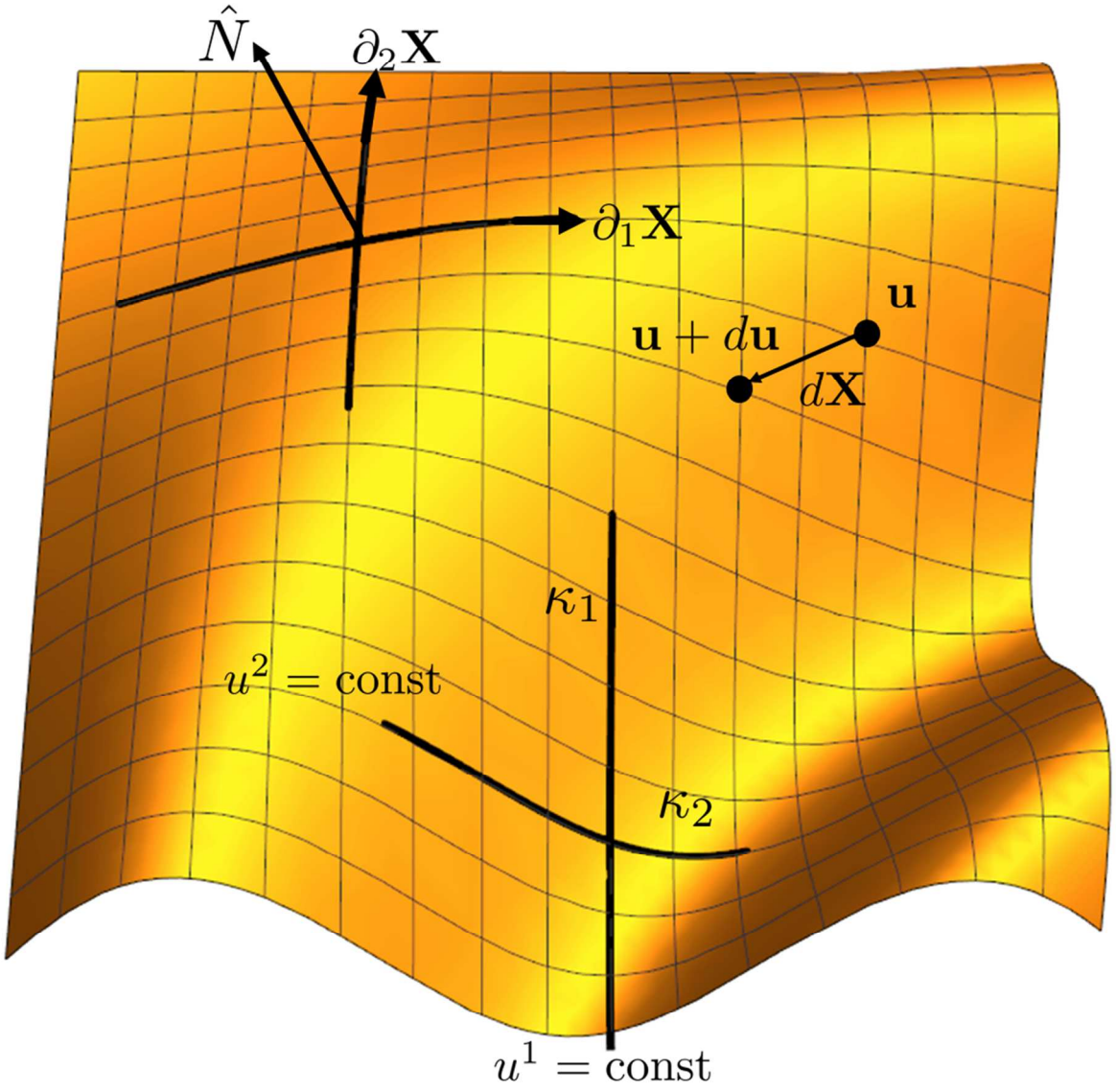
$\hat{N}$
$\partial_2 \mathbf{X}$
$\partial_1 \mathbf{X}$
$\mathbf{u}$
$\mathbf{u} + d\mathbf{u}$
$d\mathbf{X}$
κ_1
$u^2 = \text{const}$
κ_2
$u^1 = \text{const}$

Stability of a growing cylinder under geometric and mechanical feedback mechanisms. Feedback mechanisms are constrained by symmetry and locality.